Realization of Magnetic Resonance Current Density Imaging at 3 Tesla

C. Göksu, M. Sadighi, H. H. Eroğlu, and M. Eyüboğlu, *IEEE Member*

***Abstract*— Magnetic Resonance Current Density Imaging (MRCDI) is an imaging modality, which reconstructs electrical current density distribution inside a material by using Magnetic Resonance Imaging (MRI) techniques. In this study, a current source with maximum current injection capability of 224.7mA, under 1kΩ resistive load is used. Experiments are performed with a 2D uniform phantom, in which a current steering insulator is inserted. Magnetic flux density distributions are measured, and current density images are reconstructed. The reconstructed images are in agreement with the reconstructions obtained with simulated measurements.**

I. Introduction

Reconstructing current density distribution may be useful in many biomedical engineering applications, such as improving the design of electrical stimulator, cardiac pacing, defibrillator, and electro-surgery devices [1]. Magnetic Resonance Current Density Imaging (MRCDI) is an imaging modality, which reconstructs current density distribution by using a Magnetic Resonance Imaging (MRI) platform [2].

In MRCDI, external current is injected to the imaging region in synchrony with MRI pulse sequence. Current density distribution within the object created by the external current creates a local gradient and induces an additional phase accumulation in the acquired Magnetic Resonance (MR) signal. Thus, the accumulated phase in the MR signal can be related to the magnetic flux density induced the external current. However, in order to reconstruct the current density distribution inside the imaging region, all three components of the magnetic flux density must be known. Nevertheless, only the magnetic flux density component, which is in parallel with the main magnetic field, can be measured by using MRI [2]. Therefore, each axis of the object is aligned in parallel with the main magnetic field, and the magnetic flux density component in the corresponding direction is measured. The knowledge of all three orthogonal components of the magnetic flux density due to the external current enables the reconstruction of the current density distribution inside the imaging region by using Ampere's Law [2,3].

Also, the amount of phase accumulation due to the external current is related with amplitude and pulse-width of the external current [4]. Therefore, amplitude and temporal resolution of the current source plays an important role in enhancing the quality of reconstructed current density images [5-9].

In this study, a previously developed programmable current source is modified and used to realize MRCDI at 3 Tesla. Amplitude accuracy of the current source is tested for various amplitudes, under different resistive load conditions. Also, temporal accuracy of the current source is tested for various pulse-widths. MRCDI experiment is performed with a two dimensional uniform conductivity phantom with a current steering insulator. Three orthogonal components of magnetic flux density are measured, and current density images are reconstructed. In order to make comparison, the numerical simulation of the experiment is performed. The reconstructed images from measured data are compared with the simulation results.

II. Theory

In MRCDI, using a standard spin-echo pulse-sequence with a bipolar current pulse is common. The pulse-sequence is shown in Figure 1 [5].

Assuming acquired MRI signal is noise-free, the acquired signal from standard spin-echo pulse-sequence without current injection and with current injection can be expressed as given in (1) and (2), respectively,

$$S(k_x, k_y, t) = \iint_{x,y} M(x,y) e^{j(\gamma B t + k_x x + k_y y + \theta_c)} \quad (1)$$

$$S_j(k_x, k_y, t) = \iint_{x,y} M_j(x,y) e^{j(\gamma B t + \gamma B_j T_c + k_x x + k_y y + \theta_c)} \quad (2)$$

where, $M_j(x,y)$ and $M(x,y)$ are the continuous transverse magnetization with and without current injection, respectively. γ is the gyromagnetic constant, B_j and B are magnetic field inhomogeneity with and without current injection, respectively. T_c is the current pulse-width, and θ_c is the constant phase term [3].

As given in (2), the external current acts like a local gradient and cause a phase contribution in the acquired MRI signal. Applying inverse Fourier Transform to (1) and (2), the complex MRI images without and with current injection can be expressed as given in (3) and (4), respectively.

$$M(x,y) = |M(x,y)| \, e^{j(\gamma B t + \theta_c)} \quad (3)$$

$$M_j(x,y) = |M_j(x,y)| \, e^{j(\gamma B t + \gamma B_j(x,y) T_c + \theta_c)} \quad (4)$$

This project is partially funded by METU Research Grant BAP-07-02-2013-101 and Turkish Scientific and Technological Research Council (TUBITAK) Research Grant 113E301.

Cihan Göksu is with Middle East Technical University Electrical and Electronics Engineering Department, 06800, Ankara, Turkey (e-mail: cgoksu@eee.metu.edu.tr).

Mehdi Sadighi is with Middle East Technical University Electrical and Electronics Engineering Department, 06800, Ankara, Turkey (e-mail: mehdi.sadighi@metu.edu.tr).

Hasan Hüseyin Eroğlu is with TSK Rehabilitation and Care Center, 06540, Ankara, Turkey and Middle East Technical University Electrical and Electronics Engineering Department, 06800, Ankara, Turkey (e-mail: hheroglu@gata.edu.tr).

Murat Eyüboğlu is with Middle East Technical University Electrical and Electronics Engineering Department, 06800, Ankara, Turkey (Corresponding author, e-mail: bme@eee.metu.edu.tr).

978-1-4244-7929-0/14/$26.00 ©2014 IEEE

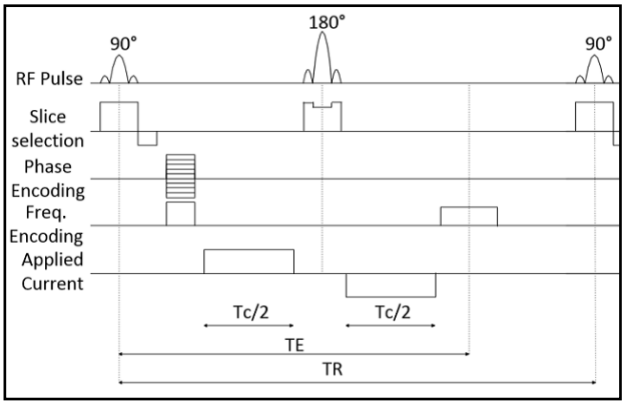

Figure 1. The spin-echo MRCDI pulse-sequence with a bipolar current pulse

Dividing (4) by (3), the induced phase due to the current can be extracted. In (3) and (4), $|M(x,y)|$ and $|M_j(x,y)|$ are equal and cancel each other. Also, θ_c term is eliminated. Therefore, the normalized phase image and magnetic flux density image due to the external current can be expressed as given in (5) and (6), respectively.

$$\emptyset_{jn}(x,y) = \gamma B_j(x,y) T_c \quad (5)$$

$$B_j(x,y) = \emptyset_{jn}(x,y)/(\gamma T_c) \quad (6)$$

In order to reconstruct the current density distribution, all three components of the magnetic flux density distribution due to the external current must be known. After measuring all three components of the magnetic flux density, the current density distribution can be reconstructed by utilizing Ampere's Law,

$$\vec{J} = (\nabla \times \vec{B})/\mu_0 \quad (7)$$

where μ_0 is the permeability of free space [3].

III. Methodology

In MRCDI, each axis of the object is aligned with the main magnetic field and MRI signal with and without current injection is acquired, separately. Reconstructed phase images are phase wrapped. Therefore, normalized phase images are reconstructed by a phase unwrapping algorithm [10]. The magnetic flux density distribution due to the current is calculated by subtracting the phase image without current from the phase image with current. Finally, current density distribution is reconstructed by taking directional derivatives of the magnetic flux density. The methodology of MRCDI is shown in Figure 2.

A. Phantom

The phantom structure is a rectangular prism. Into the structure a current steering insulator is inserted, consisting of 7 insulating parallel plates having different number of circular holes. The phantom structure and technical drawing of the phantom are shown in Figure 3 [11].

B. Current Source

The current source is composed of a microcontroller unit (MCU), a digital to analog converter (DAC), a step-up DC-DC converter, a solid state relay (SSR) driver, and a voltage to current (V-I) converter [5]. Photograph of the implemented current source is shown in Figure 4.

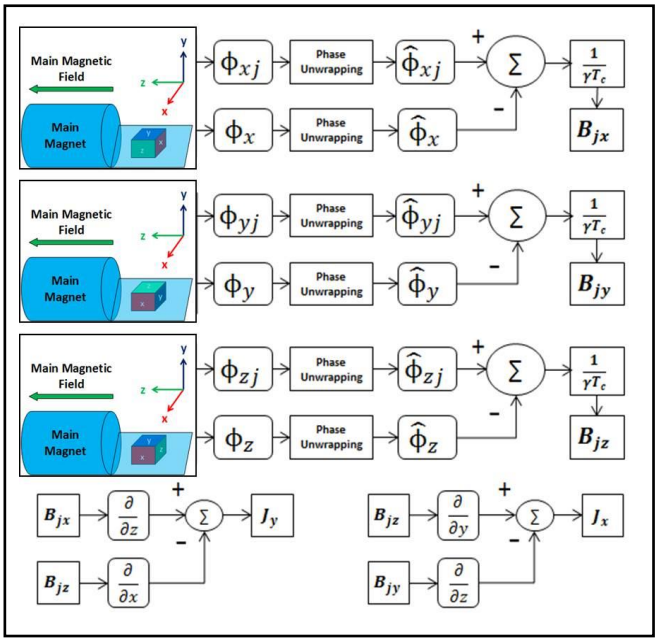

Figure 2. The methodology of MRCDI

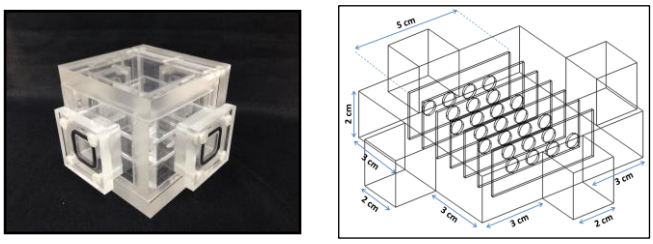

(a) (b)

Figure 3. (a) The photograph of the phantom structure, (b) Technical drawing with current simulation of the phantom [11]

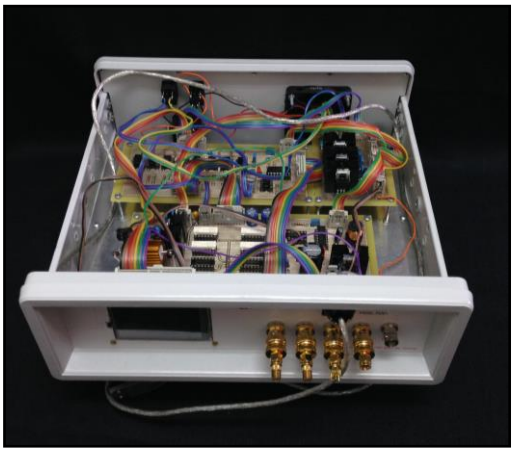

Figure 4. The photograph of the implemented current source

To operate the current source, output current parameters, which are selection of source and sink channels, amplitude, pulse-width, frequency, and delay times, are determined by the user with a graphical user interface (GUI) and the parameters are stored in the MCU. The step-up DC-DC converter generates the minimum required voltage, which feeds the V-I converter [5, 13]. Simultaneously, the MCU

generates an amplitude control signal, according to the determined amplitude, and waits for a trigger pulse. DAC converts the control signal to analog, so that V-I converter drives the current with the determined amplitude [13]. The MRI pulse sequence is designed to generate optical trigger signal for each 90° and 180° pulses in optical output of the MRI system. The optical trigger signal is converted to electrical signal, and applied to the MCU, in synchrony with RF pulses. Whenever the trigger signal is detected by the MCU, the SSR driver activates and deactivates the source and the sink channels according to the channel selection. By this way, desired current waveform is generated in synchrony with the MRI sequence, and applied repetitively during the sequence [5].

The amplitude accuracy of the current source is tested for different resistive load conditions. The desired amplitude is changed in 1mA-100mA range and the amplitude of the output current is measured. The temporal accuracy of the current source is tested, when the load is 1kΩ resistive load. The desired pulse-width is changed in 1ms-50ms range and the pulse-width of the output current is measured. The amplitude and pulse-width measurements are tabulated in Table 1 and 2, respectively.

TABLE I. AMPLITUDE MEASUREMENTS

I_{SET}/R	1 Ω	10 Ω	100 Ω	470 Ω	1 kΩ	2 kΩ
1mA	1.00	1.01	1.02	1.04	1.13	1.08
5mA	4.40	4.45	4.44	4.49	4.56	4.57
10mA	9.80	9.64	9.62	9.70	9.79	9.85
20mA	19.20	19.15	19.05	19.17	19.28	19.41
50mA	49.30	49.48	49.13	49.32	49.50	49.70
100mA	98.20	98.92	98.32	98.80	99.06	99.20

TABLE II. PULSE-WIDTH MEASUREMENTS

Δt_{SET}	1ms	5ms	10ms	20ms	50ms
Δt_{MEAS}	1.10ms	4.80ms	9.45ms	19.10ms	48.80ms
Error	10%	4%	5.5%	4.5%	2.4%

IV. EXPERIMENTAL RESULTS

The phantom shown in Figure 3, is filled with a saline solution whose conductivity is 0.2S/m, which is approximately equal to the conductivity of blood [14]. In the experiment, the standard spin-echo pulse-sequence with TR=250ms and TE=60ms is used. The voxel size is 2mm x 2mm x 5mm. 20mA-DC with 40ms pulse-width is applied. In order to increase the signal to noise ratio of the experiment, instead of performing experiment without current injection, the current is inversely applied. By this way, the accumulated phase is doubled. The magnetic flux density images with simulation results are shown in Figure 6.

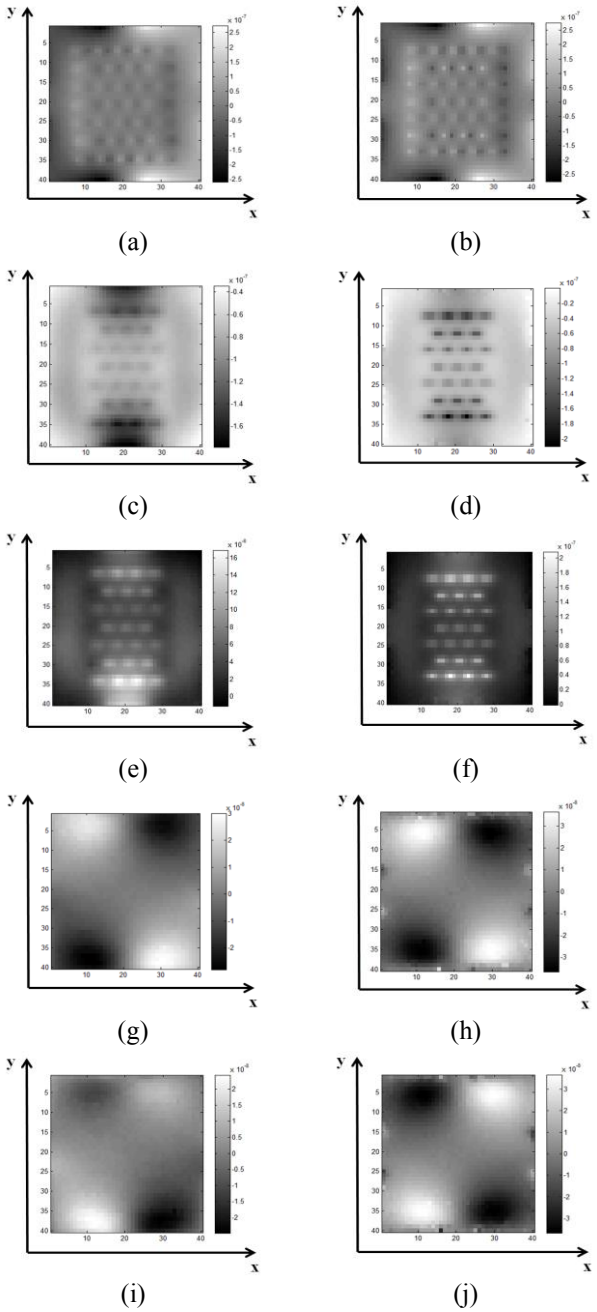

Figure 5. Measured magnetic flux density images: (a) B_z(x,y), (c) B_x^+(x,y), (e) B_x^-(x,y), (g) B_y^+(x,y), (i) B_y^-(x,y). Simulated magnetic flux density images: (b) B_z(x,y), (d) B_x^+(x,y), (f) B_x^-(x,y), (h) B_y^+(x,y), (j) B_y^-(x,y).

As shown in Figure 6, the magnetic flux density images in all directions are measured. In the magnetic flux density image, measured in transverse plane, derivative in x and y directions are calculated by forward difference. However, it is not feasible in sagittal and coronal planes. Therefore, in order to calculate the derivative in z-direction, the magnetic flux density in two consecutive slices are measured and subtracted pixel by pixel [15]. With the knowledge of measured magnetic flux density images in all directions, the current density distribution is reconstructed. The reconstructed current density images and the simulation results are shown in Figure 7.

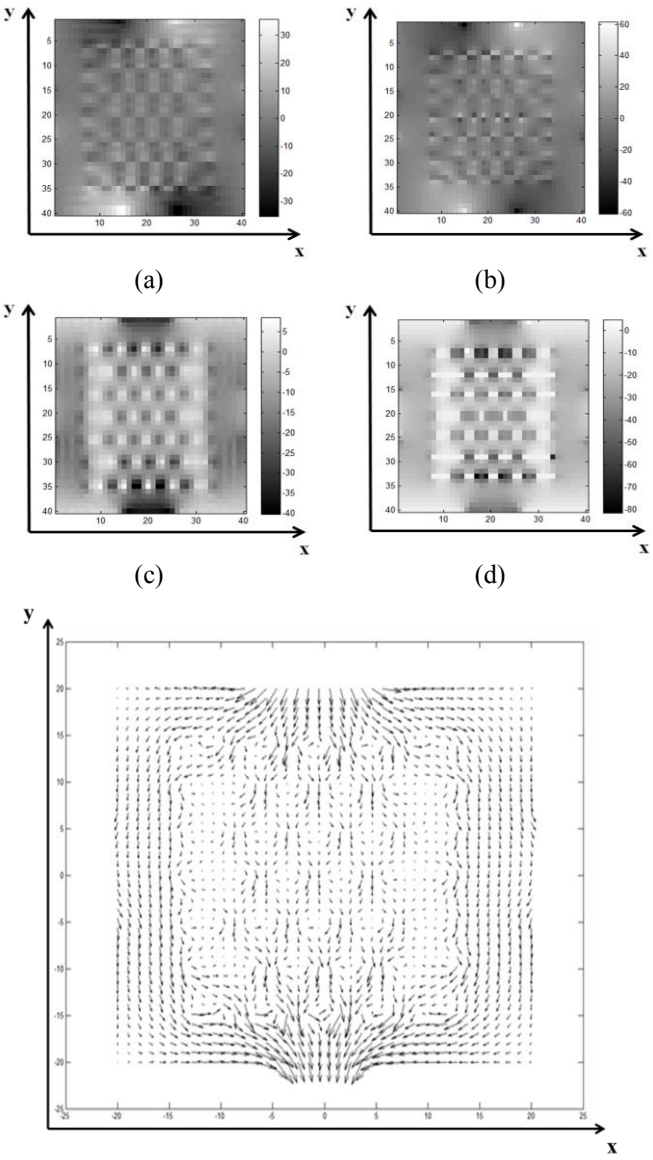

Figure 6. Current density images reconstructed from the measured magnetic flux density images: (a) $J_x(x,y)$, (c) $J_y(x,y)$. Simulated current density images: (b) $J_x(x,y)$, (d) $J_y(x,y)$. (e) The arrow plot of the measured current density distribution

As shown in Figure 6 and 7, the experimental results and the simulation results are consistent. Also, in the arrow plot in Figure 7, the change in current density vectors due to the circular holes is visible. Near the electrodes, magnetic flux density and current density data are different in experimental and simulation results. This is presumed to be due to the higher current density near the electrodes than the current density in remote regions.

V. Conclusions

In this study, a previously developed current source is modified and used in MRCDI at 3 Tesla. The maximum amplitude error of the current source is 1.8mA, when the desired amplitude is 100mA to be injected to 1Ω resistive load. The maximum temporal error is 10%, when the desired pulse-width is 1ms. The current source is utilized in an MRCDI experiment with a uniform phantom in which current steering insulator is inserted. Magnetic flux density images are measured. The current density images are reconstructed, from the measured magnetic flux density images. The magnetic flux density and the reconstructed current density images are consistent with the simulation results, except differences near the electrodes. The difference is presumed to be due to the higher current density near the electrodes. The minimum measurable current density is calculated as $0.26 uA/mm^2$ [16].

References

[1] Y. Kim, J. B. Fahy, and B. J. Tupper, "Optimal electrode designs for electrosurgery, defibrillation, and external cardiac pacing," *IEEE Trans. Biomed. Eng.*, vol. 33, no. 9, pp. 845–53, 1986.

[2] G. C. Scott and M. L. G. Joy, "Measurement of nonuniform current density by magnetic resonance," *IEEE Trans. Med. Imaging*, vol. 10, no. 3, pp. 362–374, 1991.

[3] B. M. Eyüboğlu, "MAGNETIC RESONANCE CURRENT DENSITY IMAGING," *WILEY-Encyclopedia Biomed. Eng. (Metin Akay, ed.)*, vol. 4, pp. 2147–2153, 2006.

[4] G. C. Scott, M. L. G. Joy, R. L. Armstrong, and R. M. Henkelman, "Sensitivity of magnetic-resonance current-density imaging," *J. Magn. Reson.*, vol. 97, no. 2, pp. 235–254, 1992.

[5] C. Göksu, B. M. Eyüboğlu, and H. H. Eroğlu, "A Programmable Current Source for MRCDI & MREIT Applications," in *XIII Mediterranean Conference on Medical and Biological Engineering and Computing 2013*, Seville, 2014, pp. 198–201.

[6] T. I. Oh, Y. Cho, Y. K. Hwang, S. H. Oh, E. J. Woo, and S. Y. Lee, "Improved Current Source Design to Measure Induced Magnetic Flux Density Distributions in MREIT," *J. Biomed. Eng. Res.*, vol. 27, no. 1, pp. 30–37, 2006.

[7] H. H. Eroğlu, B. M. Eyüboğlu, and C. Göksu, "Design and implementation of a bipolar current source for MREIT applications," in *XIII Mediterranean Conference on Medical and Biological Engineering and Computing 2013*, Seville, 2014, pp. 161–164.

[8] Y. T. Kim, P. J. Yoo, T. I. Oh, and E. J. Woo, "Development of a low noise MREIT current source," *International Conference on Electrical Bioimpedance 2010*, Florida, 2010.

[9] M. Goharian, K. Chin, and G. R. Moran, "A Novel Microcontroller Current Driver Design for Current Density Imaging," in *International Society for Magnetic Resonance in Medicine 2005*, Miami, 2005, pp. 2352.

[10] Z. Liang, "A Model-Based Method for Phase Unwrapping," *IEEE Trans. Med. Imaging*, vol. 15, no. 6, pp. 893–897, 1996.

[11] M. Sadighi, "Magnetic Resonance Current Tensor Imaging (MRCTI) in 3T MRI System," M.S. thesis, METU EEE Dep., 2014.

[12] S. S. Deswal, R. Dahiya, and D. K. Jain, "Application of Boost Converter for Ride-through Capability of Adjustable Speed Drives during Sag and Swell Conditions," in *World Acad. Sci. Eng. Technol.*, 2008, pp. 282–286.

[13] A. Devices, *Circuit Note CN-0151, Versatile High Precision Programmable Current Sources Using DAC's, Op Amps, and MOSFET Transistors*, 2011.

[14] C. Gabriel, S. Gabriel, and E. Corthout, "The dielectric properties of biological tissues: I. Literature survey.," *Phys. Med. Biol.*, vol. 41, no. 11, pp. 2231–49, Nov. 1996.

[15] C. Göksu, "A Programmable Current Source for MRCDI at 3 Tesla," M.S. thesis, METU EEE Dep., 2014.

[16] C. Göksu, M. Sadighi, and B. M. Eyüboğlu, "Minimum Measurable Current Density with MRCDI at 3 Tesla," in *International Symposium on Biomedical Imaging 2014*, accepted.